



*Republic of Iraq Ministry of Higher Education
and Scientific Research
University of Diyala
College of Science
Department of Physics*



Fabrication and Characterization of Perovskite Nanostructured Multijunction Solar Cells

A Thesis

Submitted to the Council of College of Science
University of Diyala in Partial Fulfillment of the
Requirements for the Degree of Doctor of Philosophy
in Physics

By

Shaimaa Mufeed Jassim

B.Sc. in Physics, 2007

M.Sc. in Physics, 2017

Supervised by

**Prof. Dr.
Nabeel Ali Bakr**

**Chief Researchers. Dr.
Falah Ibrahim Mustafa**

2020 A.D.

1442 A.H.

بِسْمِ اللَّهِ الرَّحْمَنِ الرَّحِيمِ

هُوَ الَّذِي جَعَلَ الشَّمْسَ ضِيَاءً
وَالْقَمَرَ نُورًا وَقَدَّرَهُ مَنَازِلَ
لِتَعْلَمُوا عَدَدَ السِّنِينَ
وَالْحِسَابَ مَا خَلَقَ اللَّهُ ذَلِكَ إِلَّا
بِالْحَقِّ يُفَصِّلُ الْآيَاتِ لِقَوْمٍ
يَعْلَمُونَ

(يونس - آية 5)

DEDICATION

To:

*The teacher and the source of human knowledge of
our Prophet Muhammad (peace be upon him)*

To:

*The lights of my life
My father and my mother*

To:

The soul of my beloved brother (Muhammad)

To:

*The lights of my eyes
Brothers and sisters*

To:

*My beloved country Iraq
The martyrs of Iraq with all the love and
appreciation*

Acknowledgment

*First of all, I would like to thank **ALLAH** for his generosity and mercy in giving the strength and the ability to complete my studies successfully and sincerest words of thanks to Prophet **Muhammad** (peace and blessings of Allah be upon him) who is forever a torch of guidance and Knowledge for the humanity.*

*I would like to express my sincere appreciation and deep gratitude to my supervisors, **Prof. Dr. Nabeel A. Bakr** and **Dr. Falah I. Mustafa** for suggesting the topic of this thesis, guidance, suggestions and continuous encouragement throughout the research work.*

*Special thanks to the Dean of the College of Science, **Prof. Dr. Tahseen H. Mubarak** and the head of the Physics Department, **Prof. Dr. Ziad T. Khodair** and all the Staff of the Department of Physics for their assistance.*

*Special thanks to **Dr. Abdulrahman K. Ali** in the University of Technology for helping me. Also, My thanks and gratitude are extended to the Head of the department of hydrogen and bio-fuel where, **Dr. Kiffah Al-Amara** for guidance and help throughout this work.*

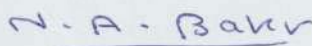
*My thanks also are extended to the staff of the Solar Cells laboratory in the Science and Technology Ministry, especially **Dr. Aqel M. Jafar** for guidance throughout this work and their help.*

My thanks go my family for their unwavering support through the whole adventure; I could not have done it without them (my father, my mother).

*Finally, I thank all my classmates and I wish them success and I would also express my deep sense of gratitude to **Shahlaa Munther** and **Widean Kadim**.*

Supervisor Certification

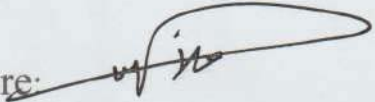
We certify that this thesis entitled "*Fabrication and Characterization of Perovskite Nanostructured Multijunction Solar cells*" submitted by "*Shaimaa Mufeed Jassim*", was prepared under our supervision at the Department of Physics, College of Science, University of Diyala in partial fulfillment of requirements needed to award the Degree of Doctor of Philosophy (Ph.D.) in Physics.

Signature: 

Name: **Dr. Nabeel A. Bakr**

Title: Professor

Date: 1 / 12 /2020

Signature: 


Name: **Dr. Falah I. Mustafa**

Title: Chief Researchers

Date: 1 / 12 /2020

Head of the Physics Department

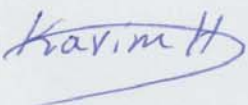
In view of the available recommendation, I forward this thesis for debate by the examining committee.

Signature: 

Name: **Dr. Ziad T. Khodair**

Linguistic Amendment

I certify that the thesis entitled "**Fabrication and Characterization of Perovskite Nanostructured Multijunction Solar Cells**" presented by (*Shaimaa Mufeed Jassim*) has been corrected linguistically, therefore, it is suitable for debate by examining committee.

Signature: 

Name: Dr. Karim H. Hassan

Title: Professor .

Address: University of Diyala/ College of Science/ Department of Chemical

Date: 30/11/2020

Scientific Amendment

I certify that the thesis entitled "**Fabrication and Characterization of Perovskite Nanostructured Multijunction Solar Cells**" presented by (*Shaimaa Mufeed Jassim*) has been evaluated scientifically, therefore, it is suitable for debate by examining committee.

Signature:

A handwritten signature in blue ink, appearing to read "Odai", written in a cursive style.

Name: Dr. Odai N. Salman

Title: Assistant Professor


Address: University of Technology / Applied Science Department

Date: 29 / 11 /2020

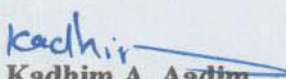
Examination Committee Certificate

We certify, that we have read the thesis entitled "**Fabrication and Characterization of Perovskite Nanostructured Multijunction Solar Cells**", presented by (**Shaimaa Mufeed Jassim**) and as an examining committee, we examined the student on its contents, and in what is related to it, and that in our opinion it meets the standard of a thesis for the Degree of **Doctor of Philosophy (Ph.D.) in Physics Sciences**.


(Chairman)

Signature: 
Name: **Dr. Ziad T. Khodair**
Title: **Professor**
Date: **20 / 11 / 2020**


(Member)

Signature: 
Name: **Dr. Kadhim A. Aadim**
Title: **professor**
Date: **2 / 12 / 2020**

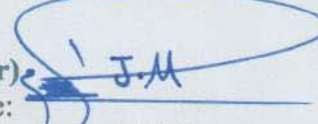
(Member)

Signature: 
Name: **Dr. Abdulsamee F. Abdul Aziz**
Title: **Professor**
Date: **2 / 12 / 2020**

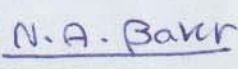
(Member)

Signature: 
Name: **Dr. Osama A. Dakhil**
Title: **Assistant Professor**
Date: **3 / 12 / 2020**

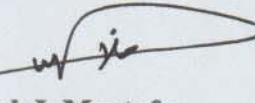
(Member)

Signature: 
Name: **Dr. Jasim M. Mansoor**
Title: **Assistant Professor**
Date: **30 / 11 / 2020**

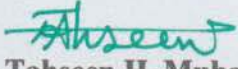
(Supervisor)

Signature: 
Name: **Dr. Nabeel A. Bakr**
Title: **Professor**
Date: **1 / 12 / 2020**

(Supervisor)

Signature: 
Name: **Dr. Falah I. Mustafa**
Title: **Chief Researchers**
Date: **1 / 12 / 2020**

Approved by the Council of the College of Science
(The Dean)

Signature: 
Name: **Dr. Tahseen H. Mubarak**
Title: **Professor**
Date: **7 / 12 / 2020**

Abstract

Perovskite and Multijunction solar cells are a third generation type of solar cells. Their working principle is based on the conversion of sunlight into electrical energy.

In this study, firstly three types of methyl ammonium halide nanopowders MAX (X = halide= I, Br, and Cl) have been synthesized by using chemical bath method. After that, eight different types of organic-inorganic perovskite thin films have been prepared by using spin coating technique which is (MAPbI₃, MAPbBr₃, MAPbCl₃, MAPbICl₂, MAPbIBr₂, FAPbI₃, CsPbI₃ and MASnCl₃). In addition, eight single inverted planar perovskite solar cells (SIPPSCs) and multijunction inverted solar cells (MJISCs (c-Si and SIPPSCs)) have been fabricated successfully by using the prepared different perovskite films as a sensitized absorption layer (active layer).

The structure of SIPPSC consisted of (fluorine tin oxide (FTO) substrate/ Poly (3,4-ethylenedioxythiophene) polystyrene sulfonate (PEDOT:PSS)/ Perovskite/ [6,6]-Phenyl C₇₁ butyric acid methyl ester (PC₇₁BM)/ Aluminum (Al)). In beginning, PEDOT: PSS layer was deposited on FTO coated glass substrate by spin coating technique which acts as hole transport layer (HTL). The different types of perovskite material that act as an absorbing layer were deposited on PEDOT: PSS layer also by spin coating technique. Then, PC₇₁BM layer which represents the electron transport layer (ETL) was deposited on perovskite layer by spin coating technique. Finally, Al as a metal layer was deposited on PC₇₁BM film by thermal evaporation technique, to get cathode electrode.

MJISC structure consisted of (Al/ crystal-silicon (c-Si)/ tin oxide (SnO_2)/ PC_{71}BM / Perovskite/ PEDOT: PSS/ FTO). For the fabrication of MJISCs, initially the SnO_2 as a transparent layer was deposited on the c-Si solar cell by using thermal evaporation technique. Then (Al) was deposited as a conductive electrode on the back face of the silicon cell also by using thermal evaporation technology. Finally, the single inverted perovskite solar cell without Al layer was stacked on c-Si solar cell with SnO_2 film by using simple mechanical method.

The structural and morphological properties of prepared powders, different perovskite thin films and SnO_2 film have been investigated by X-ray diffraction (XRD) and field emission scanning electron microscope (FESEM) techniques respectively. The optical properties (absorbance and energy gap) of different perovskite films, SnO_2 and PEDOT: PSS films have been investigated by (UV-Vis) spectrophotometer. While, photovoltaic characterizations of the fabricated IPPSCs and MJISCs based on different perovskite films have been measured by solar cell simulator.

The XRD results showed that all powders and SnO_2 film were polycrystalline with tetragonal structure. All the perovskite films were polycrystalline with different structures which are (tetragonal MAPbI_3 , cubic (MAPbBr_3 , MAPbCl_3 , MAPbICl_2 and MAPbIBr_2), rhombohedral FAPbI_3 , orthorhombic CsPbI_3 and triclinic MASnCl_3).

The FESEM images showed that the powders possess nanonails at (X= I) and nanospheres at (X= Br and Cl) like shapes. While, the perovskite films possess different shapes and SnO_2 film has cauliflower like shapes.

The results of UV-Vis spectra showed that all perovskite films have a good absorbance in visible and near IR region. Consequently, it was chosen as an active absorption layer in applications of solar cell.

The optical energy gap for allowed direct electronic transition was calculated using Tauc's model and it was found that the values of energy gap of all perovskite films vary with different variables.

The photo current density-voltage (J-V) curve characteristics of fabricated solar cells have been measured under simulated solar light (100 mW/cm^2). On the other hand, the parameters (including V_{oc} , J_{sc} , FF and efficiency) of solar cells were calculated depending on J-V curve.

The results showed that the fabricated SIPPSCs and MJISCs based on perovskite (methylammonium lead iodide (MAPbI_3)) layer as an active layer recorded higher efficiency of (10% and 12.8%) compared to the other fabricated solar cells.

Table of Contents

Subject	Page No.
Table of Contents	I
List of Abbreviations	VII
List of Abbreviations of Chemical Materials	X
List of Symbols	XII
List of Figures	XIV
List of Tables	XX

Item No.	Subject	Page No.
<i>Introduction & Literature Review</i>		
1.1	Introduction	1
1.2	Literature Review	3
1.3	Objectives of the Study	9
<i>Chapter Two: Theoretical Part</i>		
2.1	Introduction	10
2.2	Photovoltaic Effect	10
2.3	The Solar Spectrum	11

2.3.1	The Air Mass (AM)	12
2.4	The Solar Cell	13
2.5	Generations of Solar Cells	14
2.5.1	First Generation Photovoltaics	15
2.5.2	Second Generation Photovoltaics	15
2.5.3	Third Generation Photovoltaics	16
2.5.4	Fourth Generation Photovoltaics	16
2.6	The Semiconductor Materials	18
2.6.1	Inorganic Semiconductors	18
2.6.2	Organic Semiconductors	19
2.7	Hybrid Organic–Inorganic Semiconductors	19
2.8	Perovskite Material	19
2.8.1	Structure of Perovskite	20
2.9	Classification of Perovskite System	21
2.9.1	Halide Perovskite (ABX ₃)	22
2.9.2	Oxide Perovskite (ABO ₃)	22
2.10	Preparation Methods of Hybrid Organic-Inorganic Perovskite Films	23
2.10.1	Solution Processing	23
2.10.1.1	One-Step Spin Coating	24
2.10.1.2	Two-Step Spin Coating	25
2.10.2	Vapor-Assisted Solution Process	26

2.10.3	Thermal Vapor Process	27
2.11	Perovskite Solar Cells	27
2.12	Properties of Perovskite Materials	28
2.12.1	High Absorption Coefficient	28
2.12.2	Long Carrier Diffusion Length	29
2.12.3	Easy Processing and Low Costs	30
2.13	Architectures of Perovskite Solar Cells	30
2.13.1	Mesoporous Perovskite Solar Cells (n-i-p)	31
2.13.2	Planar Perovskite Solar Cells	31
2.13.2.1	Regular Planar (n-i-p) Perovskite Solar Cells	32
2.13.2.2	Inverted Planar (p-i-n) Perovskite Solar Cells	33
2.14	Working Principle of IPPSCs	33
2.15	Crystalline Silicon Solar Cells	35
2.16	Silicon-Perovskite Multijunction Solar Cells	35
2.17	Multijunction Solar Cells Architectures	37
2.17.1	Mechanical Multijunction Solar Cells	38
2.17.2	Monolithic Multijunction Solar Cells	38
2.18	Solar Cells Characterizations	39
2.18.1	Short Circuit Current (I_{sc})	40
2.18.2	Short-Circuit Current Density (J_{sc})	40
2.18.3	Open-Circuit Voltage (V_{oc})	41

2.18.4	Maximum Voltage (V_{\max})	41
2.18.5	Maximum Current (I_{\max})	41
2.18.6	Maximum Power (P_{\max})	42
2.18.7	Fill Factor (FF)	42
2.18.8	Power Conversion Efficiency (η)	43
2.19	The Equivalent Electrical Circuit of Solar Cell	43
2.20	Optical Properties	44
2.20.1	Absorbance (A)	44
2.20.2	Optical Energy Gap (E_g)	45
2.21	Structure of Thin Film	46
<i>Chapter Three: Experimental Procedure</i>		
3.1	Introduction	48
3.2	Experimental Work	48
3.3	Materials	49
3.4	Preparation of Methyl Ammonium Halide (Iodide, Bromide, and Chloride) Powders	50
3.5	Preparation of Solutions	51
3.6	Deposition Techniques	52
3.6.1	Spin Coating Technique	52
3.6.2	Thermal Evaporation Deposition Technique	53
3.7	Drying System	54

3.8	Fabrication of Inverted Planar Perovskite Solar Cells	55
3.8.1	FTO Coated Glass Substrates Cleaning	56
3.8.2	PEDOT:PSS Layer Deposition	56
3.8.3	Perovskite Layer Deposition	57
3.8.4	PCBM Layer Deposition	58
3.8.5	Counter Electrode (Al) Deposition	58
3.9	Preparation of Multijunction Solar Cells	59
3.10	Characterization Techniques	61
3.10.1	X-Ray Diffraction (XRD)	61
3.10.2	Field Emission Scanning Electron Microscopy (FESEM)	61
3.10.3	UV-Vis Spectroscopy	62
3.10.4	Current-Voltage (I-V) Measurement System	63
<i>Chapter Four: Results & Discussion</i>		
4.1	Introduction	64
4.2	Structure Properties	64
4.2.1	XRD Analysis of (MAX) Powders	64
4.2.2	XRD Analysis of Perovskite Thin Films	68
4.3	Morphological Analysis	78
4.3.1	FESEM Analysis for Powders and Perovskite Thin Films	78

4.4	Optical Properties	87
4.5	J-V Characterizations of Perovskite and Multijunction Solar Cells	102
4.6	Conclusions	111
4.7	Future Works	111
References		112

List of Abbreviations

Abbreviation	Definition
0D	Zero dimension
1D	One dimension
2D	Two dimension
2-T	2-Terminal
4GSCs	Fourth Generation Solar Cells
4-T	4-Terminal
ABO₃	Oxide Perovskite
ABX₃	Halide Perovskite
AM	Air Mass
AM0	The solar radiation spectrum outside of the earth's atmosphere
AM1	The distance of the solar radiation spectrum required to reach the earth's surface when the sun is directly at an overhead position relative to the earth
AM1.5	Solar radiation at the earth's surface when the solar rays make an angle of 48.2° with the vertical
a-Si	Amorphous Silicon
CB	Conduction Band
CIGS	Copper Indium Gallium Selenide
c-Si	Crystalline Silicon

DEE	Diethyl ether
DIW	Diionized water
DMF	N,N dimethyl formamide
DMSO	Dimethyl Sulfoxide
DSSCs	Dye Sensitized Solar Sells
ETL	Electron Transport Layer
FESEM	Field Emission Scanning Electron Microscopy
FTO	Fluorine–doped Tin Oxide
FWHM	Full Width at Half Maximum
GBL	Gamma-Butyrolactone
HIT	Hetero-Junction with Intrinsic Thin Layer
HOMO	Highest Occupied Molecular Orbital
HTL	Hole Transport Layer
ICDD	International Center of Diffraction Data
I-V	Current-Voltage
J-V	Current density–Voltage
LUMO	Lowest Unoccupied Molecular Orbital
MA	Methyl amine
MJISCs	Multijunction Inverted solar cells
MPP	Maximum Power Point
PC₇₁BM	[6,6]-Phenyl C ₇₁ Butyric Acid Methyl Ester
PCBM	[6,6]-Phenyl Butyric Acid Methyl Ester
PCE	Power Conversion Efficiency

PEDOT:PSS	Poly(3,4-ethylenedioxythiophene) Polystyrene Sulfonate
PHJPSCs	Planar Hetero-Junction Perovskite Solar Cells
PHSCs	Planar Hetero-Junction Solar Cells
PSCs	Perovskite Solar Cells
PTAA	Poly [bis(4-phenyl)(2,4,6-trimethylphenyl)amine]
PV	Photovoltaic
R_s	Series resistance
R_{sh}	Shunt resistance
SIPPSCs	Single Inverted planar perovskite solar cells
TCO	Transparent Conductive Oxide
TFSC	Thin Film Solar Cell
TSCs	Tandem Solar Cells
UV-Vis	Ultraviolet-Visible
VB₁	Initial Valence Band
VB₂	Second Valence Band
VB₃	Third Valence Band
XRD	X-Ray Diffraction

List of Abbreviations of Chemical Materials

Chemical Material	Definition
CaTiO₃	Calcium titanium oxide
CdTe	Cadmium telluride
CO₂	Carbon dioxide
CsI	Cuprous iodide
CsPbI₃	Cesium lead triiodide
CuI	Copper iodide
CuO	Copper oxide
CuSCN	Cuprous thiocyanate
FAI	Formamidinium iodide
FAPbI₃	Formamidinium lead triiodide
HBr	Hydrobromic acid
HCl	Hydrochloric acid
HF	Hydrofluoric acid
HI	Hydroiodic acid
MABr	Methyl ammonium bromide
MACl	Methyl ammonium chloride

MAI	Methyl ammonium iodide
MAPbBr₃	Methyl ammonium lead tribromide
MAPbI₃	Methyl ammonium lead triiodide
MASnCl₃	Methyl ammonium tin trichloride
NiO	Nickel oxide
PbBr₂	Lead bromide
PbCl₂	Lead chloride
PbI₂	Lead iodide
SnCl₂	Tin chloride
SnO₂	Tin dioxide
V₂O₅	Vanadium pentaoxide

List of Symbols

Symbol	Meaning	Units
A	Absorbance	-
<i>a, b and c</i>	Lattice constants	Å
c	Speed of light	m/s
D	The crystallite size	nm
d_{hkl}	Interplanar spacing	Å
E	Energy of the photon	eV
e^-	Electron	-
E_g	Optical Energy Gap	eV
F.F	Fill Factor	-
h	Planck 's constant	J/s
h^+	Hole	
<i>hkl</i>	Miller indices	-
$h\nu$	Photon energy	J
I	Incident light intensity	mW/cm ²
I_D	Diode current	mA
I_E	Electric current	mA
I_L	Light induced current	mA
I_{max}	Maximum current	mA
I_o	The saturation current density	mA

I_{ph}	The light-generated current density	mA
I_{SC}	Short circuit current	mA
I_{Sh}	Shunt current	mA
I_T	Transmitted light intensity	mW/cm ²
J_{max}	Current density at maximum power point	mA/cm ²
J_{SC}	Short-circuit current density	mA/cm ²
K_B	Boltzmann constant	J/K
B	Constant	-
\dot{n}	The diode ideality factor	-
η	Efficiency	-
P_{in}	The incident power	mW/cm ²
P_{max}	Maximum power	mW/cm ²
q	The electron charge	-
r	The exponent	-
T	The temperature	K
T	Transmittance	-
V	Voltage	V
V_{max}	Maximum voltage	V
V_{oc}	Open-circuit voltage	V
α	Optical absorption coefficient	cm ⁻¹
θ_z	Solar zenith angle	Degree
λ	Wavelength of the photon	nm

n	Integer number	-
\mathcal{A}	The active surface area of the cell	cm ²
\mathcal{K}	Scherrer's constant	-
θ	Bragg's angle	degree
λ_x	The wavelength of the incident X-ray	nm
β	Full width at half maximum	rad

List of Figures

Fig. No.	Figure Caption	Page No.
2.1	Solar spectrum, and the spectrum of a black body at T=5800 K	12
2.2	The variation of air mass to zenith of sun	13
2.3	Cross-section of a basic solar cell	14
2.4	The generations of solar cells	14
2.5	Multijunction solar cell	17
2.6	Progression of efficiencies for a variety of PV technologies	17
2.7	General perovskite structure and commonly used materials	21
2.8	Types of perovskite crystal structure	21
2.9	Classification of perovskite system	22

2.10	Schematic diagram of one-step spin coating process	24
2.11	Schematic diagram of (a) Two-step spin coating and (b) Dip coating process	25
2.12	Schematic diagram of vapor-assisted solution process	26
2.13	Efficiency evolution of the perovskite solar cells	28
2.14	Absorption spectrum of MAPbI ₃ , GaAs and c-Si, showing a sharp absorption edge and high absorption coefficient for MAPbI ₃	29
2.15	Schematic diagram of a mesoporous structure PSCs	31
2.16	Schematic diagram of regular planar (n-i-p) structure	32
2.17	Schematic diagram of inverted (p-i-n) structure	33
2.18	Schemes of (a) device architecture of inverted planar (p-i-n) PSCs, and (b) the corresponding energy levels of the materials	34
2.19	Schemes of perovskite/silicon tandem solar cells architectures: (a) and (b) (2T and 4T) mechanically stacked, and (c) (2-T) monolithically integrated	37
2.20	Typical current density-voltage characteristic of solar cell	39
2.21	Equivalent electrical circuit of (a) Ideal and (b) Real solar cells	43
2.22	Effect of (a) increasing series and (b) reducing parallel resistances	44
3.1	The diagram of the experimental work	48
3.2	Photographs of MAI preparation steps	50
3.3	(a) Photograph of spin coater instrument used and (b) steps of spin coating on substrate.	53
3.4	Schematic diagram of the thermal evaporation	53

	system used	
3.5	Schematic diagram of drying system used	54
3.6	Flowchart of IPPSCs preparation steps	55
3.7	Chemical structure of PEDOT:PSS	56
3.8	Chemical structure of PC ₇₁ BM	58
3.9	Schematic diagram of shadow mask	58
3.10	Final image of IPPSC before test	59
3.11	Schematic of (a) multijunction inverted solar cell and (b) corresponding energy levels of the materials	60
3.12	Schematic diagram of X-ray diffraction	61
3.13	Schematic diagram of FESEM device	62
3.14	Schematic diagram of UV-Vis spectrophotometer	62
3.15	Schematic diagram of (I-V) measurement system	63
4.1	XRD pattern of MAI powder	65
4.2	XRD pattern of MABr powder	66
4.3	XRD pattern of MACl powder	67
4.4	XRD pattern of MAPbI ₃ film	69
4.5	XRD pattern of MAPbBr ₃ film	70
4.6	XRD pattern of MAPbCl ₃ film	71
4.7	XRD pattern of commercial MAPbICl ₂ film	72
4.8	XRD pattern of MAPbIBr ₂ film	73
4.9	XRD pattern of FAPbI ₃ film	74
4.10	XRD pattern of CsPbI ₃ film	75
4.11	XRD pattern of MASnCl ₃ film	76

4.12	XRD pattern of SnO ₂ film	77
4.13	FESEM images of MAI powder at (a) 25 kx and (b) 100 kx magnifications	78
4.14	FESEM images of MABr powder at (a) 50 kx and (b) 200 kx magnifications	79
4.15	FESEM images of MAcl powder at (a) 100 kx and (b) 200 kx magnifications	80
4.16	FESEM images of MAPbI ₃ thin film at (a) 25 kx and (b) 100 kx magnifications	81
4.17	FESEM images of MAPbBr ₃ thin film at (a) 25 kx and (b) 120 kx magnifications	81
4.18	FESEM images of MAPbCl ₃ thin film at (a) 5 kx and (b) 100 kx magnifications	82
4.19	FESEM images of commercial MAPbICl ₂ thin film at (a) 50 kx and (b) 100 kx magnifications	83
4.20	FESEM images of MAPbIB ₂ thin film at (a) 100 kx and (b) 200 kx magnifications	84
4.21	FESEM images of FAPbI ₃ thin film at (a) 50 kx and (b) 100 kx magnifications	85
4.22	FESEM images of CsPbI ₃ thin film at (a) 25 kx and (b) 200 kx magnifications	86
4.23	FESEM images of MASnCl ₃ thin film at (a) 100 kx and (b) 200 kx magnifications	86
4.24	FESEM images of SnO ₂ thin film at (a) 100 kx and (b) 200 kx magnifications	87
4.25	Absorption spectrum of PEDOT:PSS thin film	88
4.26	Tauc's plot of PEDOT:PSS thin film	88
4.27	Absorption spectrum of SnO ₂ thin film	89

4.28	Tauc's plot of SnO ₂ thin film	90
4.29	Absorption spectrum of MAPbI ₃ thin film	91
4.30	Tauc's plot of MAPbI ₃ thin film	92
4.31	Absorption spectrum of MAPbBr ₃ thin film	93
4.32	Tauc's plot of MAPbBr ₃ thin film	93
4.33	Absorption spectrum of MAPbCl ₃ thin film	94
4.34	Tauc's plot of MAPbCl ₃ thin film	94
4.35	Absorption spectrum of commercial MAPbICl ₂ thin film	95
4.36	Tauc's plot of commercial MAPbICl ₂ thin film	96
4.37	Absorption spectrum of MAPbIBr ₂ thin film	97
4.38	Tauc's plot of MAPbIBr ₂ thin film	97
4.39	Absorption spectrum of FAPbI ₃ thin film	98
4.40	Tauc's plot of FAPbI ₃ thin film	98
4.41	Absorption spectrum of CsPbI ₃ thin film	99
4.42	Tauc's plot of CsPbI ₃ thin film	100
4.43	Absorption spectrum of MASnCl ₃ thin film	101
4.44	Tauc's plot of MASnCl ₃ thin film	101
4.45	J-V curves of single perovskite solar cell and multijunction (Si/Ps) solar cell based on MAPbI ₃ as active layer	104
4.46	J-V curves of single perovskite solar cell and multijunction (Si/Ps) solar cell based on MAPbBr ₃ as active layer	105
4.47	J-V curves of single perovskite solar cell and multijunction (Si/Ps) solar cell based on MAPbCl ₃ as	105

	active layer	
4.48	J-V curves of single perovskite solar cell and multijunction (Si/Ps) solar cell based on MAPbCl ₂ as active layer	107
4.49	J-V curves of single perovskite solar cell and multijunction (Si/Ps) solar cell based on MAPbBr ₂ as active layer	107
4.50	J-V curves of single perovskite solar cell and multijunction (Si/Ps) solar cell based on FAPbI ₃ as active layer	108
4.51	J-V curves of single perovskite solar cell multijunction (Si/Ps) solar cell based on CsPbI ₃ as active layer	110
4.52	J-V characterization of single perovskite solar cell multijunction (Si/Ps) solar cell based on MASnCl ₃ as active layer	110

List of Tables

<i>Table No.</i>	<i>Table caption</i>	<i>Page No.</i>
2.1	Some inorganic semiconductors	18
3.1	The materials used to prepare solar cells	49
3.2	The material quantities to prepare MAI, MABr and MACl powders	51
3.3	The required parameters to prepare the solutions	51
3.4	The required parameters to prepare thin films by thermal evaporation deposition technique	54
3.5	Preparation of perovskite thin films by two-step spin coating method	57
3.6	The different structures of types of fabricated solar cells	60
4.1	X-ray diffraction results of prepared powders and thin films	77
4.2	The photovoltaic parameters of the solar cells fabricated by using different perovskite films	101

Chapter One

Introduction & Literature Review

1. Introduction

The increase in industrialization and rapid growth in human population is envisaged to intensify the demand for energy in the near future by a significant proportion [1]. The primary source of energy fossil fuel, which accounted for 66.7% of the world energy consumption has been predicted to exhaust in supply sooner or later. Also, the primary source of energy does produce carbon dioxide (CO₂), which has been identified as the main cause of global warming [2]. Therefore, substantial scientific researchers have been focusing on developing a greener and more sustainable energy to alleviate the environmental impacts [3]. Photovoltaic (PV) is a technology that uses semiconducting materials that exhibit photovoltaic effects and convert sunlight into electricity [4]. Due to abundance, low cost, and environmental friendliness, solar energy has gained significant attention as an outstanding candidate for future power generation [5]. The solar energy is the most promising because of its enormous theoretical and technical potential. The amount of energy from sunlight striking the earth in 1 hour is about (4.3×10^{20} J), which is higher than all of the energy currently consumed on the planet in one year (4.1×10^{20} J) [1]. Solar cells can be used as an alternative and renewable energy source that are able to convert light into electric current, both the direct sun light and also artificial light, together with no noise, pollution or moving parts, making them robust, reliable, and long lasting [6]. A new generation of organic-inorganic halide perovskite emerged to prominence in the past few years. Comparing to conventional silicon solar cell, the perovskite-based solar cell has a higher energy return on investment due to low material utilization and ability to the solution process [7]. The efficiency of perovskite solar cells (PSCs) has increased up from 3.8% in 2009 to 23.9% in 2019 [8].

Crystalline silicon (c-Si) solar cells have achieved enormous dominance in the photovoltaic market due to their high efficiencies, excellent material quality, near-optimal band gap energy, and reduction in manufacturing costs [9]. c-Si solar cells are approaching their theoretical Auger limit of 29.4% with a current record at 26.7%. One promising approach to overcome this limit relies on reducing thermalization losses by stacking several absorbers of different band gaps together in a multi-junction or tandem device [10]. Tandem solar cells (TSCs) have been proposed to achieve higher conversion efficiency than single-junction solar cells [11]. TSCs are multijunction photovoltaic devices, a unique combination of two sub-cells that arranging in form top solar cell (high band gap) and bottom solar cell (low band gap) that stacked on top of each other [12]. The band gap of the top sub-cell is required to be higher than the band gap of silicon (1.1 eV) in order to absorb the photons of higher energy, thus yielding two complementary absorbing subcells [13]. The incident sunlight first hits the top cell which has a higher band gap and harvests the high-energy photons at a higher voltage, while the low-energy photons are transferred to the bottom cell which has a lower band gap and corresponding lower voltage [14]. In this way, high-energy photons are able to contribute more voltage to the device instead of losing their excess energy by thermalization [15]. Organic-inorganic perovskite materials are excellent photovoltaic materials for tandem applications due to strong absorption coefficients, long electron-hole diffusion lengths, tunable band gap, high charge carrier mobilities, solution-processable, and low cost [16, 17]. As a result, tandem cells with a perovskite top cell and a silicon bottom cell have the potential to reach efficiencies beyond 30%. Consequently, the tandem structure has been proved to be an efficient method to enhance the efficiency of organic or other types of solar cells.

Organic-inorganic perovskite and c-Si solar cells are fabricated in mainly two configurations: mechanically stacked 4-terminal (4-T) tandem and monolithic 2-terminal (2-T) tandem [18]. TSCs are promising results that have been achieved for 2-T and 4-T perovskite/silicon tandem solar cells reaching energy conversion efficiencies of up to 23.6% and 26.4%, respectively [19].

1.2 Literature Review

In 2009, Kojima et al. prepared two types of perovskite methyl ammonium lead triiodide (MAPbI₃) or CH₃NH₃PbI₃) and methyl ammonium lead tribromide (MAPbBr₃ or CH₃NH₃PbBr₃) by chemical bath method to fabricate solar cells. Perovskite solar cells were fabricated in the structure of order (TiO₂/MAPbI₃ or MAPbBr₃/Spiro-MeOTAD). The solar cell based on MAPbI₃ obtained results of short circuit current density (J_{sc}), open-circuit voltage (V_{oc}), fill factor (F.F), and power conversion efficiency (PCE) were equal to 11 mA.cm⁻², 0.61 V, 0.57, and 3.81%, respectively. While, the solar cell based on MAPbBr₃ recorded J_{sc}=5.75 mA.cm⁻², V_{oc}=0.96 V, F.F=0.59 and PCE=3.13% respectively [20].

In 2011, Im et al. fabricated quantum dot sensitized solar cell based on MAPbI₃ material as an active layer with the following structure (TiO₂/MAPbI₃/ Pt). Spin coating method was used to deposit MAPbI₃ thin film onto the surface of titanium oxide. From the results, it was found that efficiency of the fabricated solar cell recorded 6.54% at AM1.5 (1 sun) illumination [21].

In 2013, Kim et al. synthesized nanoparticles perovskite from the reaction of methylammonium iodide (MAI or CH₃NH₃I) with lead iodide (PbI₂) solutions. Also, perovskite solar cells were fabricated in the structure order of (TiO₂/MAPbI₃/Spiro-MeOTAD) by spin coating technique. From

the results, it was found that J_{sc} was 17 mA/cm², V_{oc} was 0.888 V, F.F. was 0.62, and PCE was 9.7% [22].

In 2013, Bi et al. synthesized CH₃NH₃PbI₃ by two-step spin coating technique for methylammonium lead iodide perovskite films for the preparation of highly reproducible solar cells, with the following structure (FTO/C-TiO₂/m-TiO₂/CH₃NH₃PbI₃/Spiro-OMeTAD/Ag). It was found that J_{sc} was 18.3 mA/cm², V_{oc} was 0.89 V, F.F. was 0.58 and efficiency reached up to 9.5% which was achieved under AM 1.5 illumination of 1000 W m⁻² [23].

In 2014, Eperon et al. fabricated planar hetero-junction perovskite solar cells (PHJPCs) with the following structure (FTO/C-TiO₂/Perovskite (CH₃NH₃PbI_{3-x}Cl_x)/Spiro-OMeTAD/Au). The perovskite layer was deposited on the surface of the C-TiO₂ film by using spin coated method. From current density-voltage (J-V) curve, it was noted that J_{sc} =15.3 mA/cm², V_{oc} =0.8 V, F.F.=0.55, and PCE= 6.7% [24].

In 2014, Eperon et al. synthesized formamidinium lead trihalide (FAPbX₃ or NH₂CH=NH₂PbX₃, X=halide= I and Br) perovskite films and showed the effect of replacing the methyl ammonium cation in this perovskite (FAPbI_zBr_{3-z}), with the slightly larger formamidinium cation, with z increasing from (0 to 1). FAPbI_zBr_{3-z} films have a band gap tunable between 1.48 and 2.23 eV, respectively. They took the 1.48 eV band gap perovskite as most suited for single junction solar cells, and demonstrated long-range electron and hole diffusion lengths in this material, making it suitable for planar hetero-junction solar cells (PHJSCs). They fabricated such devices, and due to the reduced band-gap they achieved high short-circuit currents of >23 mA/cm², resulting in power conversion efficiencies of up to 14.2%, the highest efficiency yet for solution processed PHJPCs. Formamidinium lead triiodide (FAPbI₃) was hence promising as another candidate for this class of solar cells [25].

In 2015, Chen et al. synthesized perovskite/polymer in tandem solar cell structure. The wide band gap perovskite absorber MAPbI_3 was processed via a one step deposition. It was observed that PCE of 9.1% was obtained for a single-junction, planar structured MAPbI_3 solar cell. While the hybrid tandem solar cell based on perovskite/polymer subcells could achieve an optimal efficiency of 10.2% which is greater than both of the perovskite and polymer single-junction cells [26].

In 2015, Yuan et al. fabricated inverted planar perovskite solar cells (IPPSCs) by using FAPbI_3 as a layer for light harvesting. X-ray diffraction (XRD), field emission scanning electron microscope (FESEM) and J-V curve properties of FAPbI_3 film were studied. IPPSCs were fabricated with the following structure (ITO/PEDOT:PSS/ FAPbI_3 /PCBM/BCP/Ag) by spin coating technique. From the curves, it was found that PCE of 13.56% was obtained with high short circuit current density of 21.48 mA/ cm^2 [27].

In 2015, Eperon et al. prepared inorganic perovskite material cesium lead triiodide (CsPbI_3). They also fabricated planar inverted perovskite solar cells with structure (ITO/PEDOT:PSS/Perovskite(CsPbI_3)/PCBM/Al). The XRD and Ultraviolet-Visible (UV-Vis) characterizations were carried out for synthesized CsPbI_3 thin films. From J-V characteristics, it was found that the planar inverted device generates PCE of 1.7% [28].

In 2015, Loper et al. fabricated 4-T monolithic tandem solar cell consisting of a methyl ammonium lead iodide as top cell and a c-Si as bottom cell. The tandem solar cell was fabricated in the structure order of (Ag/c-Si/c-TiO₂/m-TiO₂/Perovskite (MAPbI_3)/Spiro-MeOTAD/Ag). The MAPbI_3 top cell displayed broad band transparency owing to its design free of metallic components and yields a transmittance of >55% in the near infrared spectral region. This allowed generating a short-circuit current density of 13.7 mA/ cm^2 in the bottom cell. From the results, it was shown

that the 4-T tandem solar cell yielded an efficiency of 13.4 % (perovskite cell: 6.2 % and c-Si cell: 7.2 %) [29].

In 2015, Werner et al. fabricated monolithic perovskite/silicon hetero-junction tandem solar cells yielding efficiencies of up to 21.2 and 19.2% for cell areas of 0.17 and 1.22 cm², respectively [5].

In 2016, Ren et al. fabricated 4-T perovskite/c-Si tandem solar cells. The perovskite solar cell as top cell was consisting of (FTO/TiO₂/Perovskite(MAPbI₃)/Spiro-MeOTAD/MoO₃/Au/MoO₃). While, c-Si solar cell as bottom cell was consisting of (Al/ p-n Si/ SiNx/ Ag). The tandem cells were produced by combining the perovskite with c-Si solar cells by mechanical method. From the results, it was found that PCE of 23.6% for a multijunction device is achieved compared to 18.1% and 19.1% of individual perovskite and c-Si solar cells respectively [30].

In 2016, Albrecht et al. fabricated a monolithic tandem device formed by a silicon hetero-junction as bottom cell and a perovskite (CH₃NH₃PbI₃) as top cell. The monolithic integration was achieved via low temperature processing of the perovskite subcell where an energetically aligned electron selective contact was fabricated by atomic layer deposition of tin oxide. The hole selective transparent top contact was formed by a stack of the organic hole transport material spiro-OMeTAD, molybdenum oxide and sputtered indium tin oxide. It was recorded that the PCE of silicon, perovskite, and tandem are 15.7%, 10.4%, and 19.1% respectively [31].

In 2017, Fan et al. prepared 4-terminal tandem (Si/Ps) solar cell. The fabricated perovskite solar cell acting as the top cell was composed of (FTO/c-TiO₂/Perovskite (CH₃NH₃PbI_{3-x}Cl_x)/Spiro-MeOTAD/Au). Then the tandem cell was synthesized by combining top cell (perovskite cell) with bottom cell (crystal silicon) by simple mechanical method. From the results, it was found that the tandem solar cell yielded an efficiency of

14.8%, with contributions of the top 8.98% and the bottom cell 5.82% respectively [32].

In 2017, Suhail et al. prepared organolead halide perovskite solar cells based on ($\text{CH}_3\text{NH}_3\text{PbI}_3$, $\text{CH}_3\text{NH}_3\text{PbBr}_3$, $\text{CH}_3\text{NH}_3\text{BrPbI}_2$, $\text{CH}_3\text{NH}_3\text{IPbCl}_2$, $\text{CH}_3\text{NH}_3\text{IPbBr}_2$ and $\text{CH}_3\text{NH}_3\text{BrPbCl}_2$) as absorption layer. These cells recorded efficiency of (2.15 %, 0.74 %, 0.56 %, 0.27 %, 0.12 %, and 0.07 %) respectively [3].

In 2018, Singh et al. synthesized perovskite material methyl ammonium tin trichloride (MASnCl_3) and studied its application in fabrication of PSCs. MASnCl_3 was prepared by direct deposition of equimolar concentration of methylammonium chloride (MACl) and tin chloride (SnCl_2) in Anhydrous N,N dimethyl formamide (DMF) solution. The XRD, UV-Vis, and FESEM characterization of the prepared thin films were performed. The perovskite solar cell was fabricated in the structure order of (FTO/ b-TiO₂/ n-TiO₂/ Perovskite ($\text{CH}_3\text{NH}_3\text{SnCl}_3$)/ Electrolyte/ Pt/ FTO) by spin coating method. It was noted the fabricated perovskite solar cells showed PCE of 0.55% at 100 mW/cm² [33].

In 2018, Kanda et al. prepared perovskite single-junction solar cells and 2-T tandem solar cells. The perovskite solar cells were fabricated based on MAPbI_3 material as absorbent layer with the following structure (FTO/bl-TiO₂/m-TiO₂/ MAPbI_3 /Spiro-MeOTAD/ MoO₃). While, tandem cell was fabricated by combining silicon solar cell with perovskite solar cell in mechanically stacked form by direct contact of transparent conductive oxide (TCO) layers of each sub-cell. The photovoltaic parameters of tandem device solar cell were $J_{\text{SC}}=16.2 \text{ mA/cm}^2$, $V_{\text{OC}}=1.42 \text{ V}$, $\text{FF}=0.602$, $\text{PCE}=13.9\%$ [34].

In 2018, Pisoni et al. prepared tandem solar cell based on perovskite as top cell and Cu(In,Ga)Se₂ (CIGS) as bottom cell. The perovskite solar cell based on MAPbI₃ material as an active layer was fabricated in the structure following (IZO/C₆₀/perovskite (MAPbI₃)/Spiro-OMeTAD/Au). Then, the tandem cell was fabricated by combining the perovskite with CIGS solar cell by mechanical stacked method. It was found that perovskite cell, CIGS cell and perovskite/CIGS tandem devices were demonstrated with an efficiency of 14%, 5.6%, 19.6%, respectively [35].

In 2018, Zhuk et al. fabricated monolithic perovskite/silicon hetero-junction 2-T tandem solar cells. The perovskite solar cell with structure (FTO/SnO₂/MAPbBr₃/Spiro-OMeTAD/Au) was synthesized. From the results, it was found that perovskite solar cell and perovskite/silicon multijunction solar cell were obvious with a PCE of 14.39% and 18.42%, respectively [36].

In 2018, Bush et al. fabricated 2-T monolithic tandem solar cells. They chose the silicon as bottom cell and perovskite as top cell. In addition, the cesium formamidinium lead halide was used as an active layer in perovskite solar cells. The single-junction perovskite solar cells were fabricated in the structure order of (ITO/NiO/C_{S0.17}FA_{0.83}Pb (Br_{0.17}I_{0.83})₃/PC₆₀BM/SnO₂/ITO/LiF/Ag). The results showed that the total power conversion efficiency of tandem cell reached 23.6% [17].

In 2018, Qiu et al., synthesized four mixed perovskite thin films (FA_{0.48}MA_{0.37}CS_{0.15}PbI_{2.23}Br_{0.77}, FA_{0.57}MA_{0.43}PbI_{2.4}Br_{0.96}, FA_{0.5}MA_{0.38}CS_{0.12}PbI_{2.04}Br_{0.96} and FA_{0.51}MA_{0.38}CS_{0.11}PbI_{1.85}Br_{1.15}) with different band gaps 1.65 eV, 1.69 eV, 1.69 eV and 1.72 eV respectively by spin coating technique. Also, monolithic tandem solar cells were fabricated by using the prepared perovskite films in the following structure (Si cell/ITO/SnO₂/Perovskite/Spiro-OMeTAD/MoO_x/ITO). From the results, it was found that the perovskite film with a 1.69 eV band gap showed the best

performance when incorporated in the top subcell and consequently the resulting device achieved an efficiency of 22.2% [37].

In 2018, Baron et al. prepared two types of perovskite thin films (MAPbBr₃ and MAPbBr₂Cl) by one step coating method. The structural, morphological and optical properties of perovskite films were studied. They also fabricated single perovskite solar cells based on prepared perovskite films with the following structure (FTO/TiO₂/Ncs/MAPbX₃/Ag). From results, it was found that PCE achieved was 1.2 % and 0.9 % for MAPbBr₃ and MAPbBr₂Cl perovskite solar cells respectively [38].

In 2020, Lamanna et al. fabricated two-terminal perovskite/silicon tandem solar cell by mechanical stacking of the sub-cells. Mixed-halide perovskite (Cs_{0.06}FA_{0.78}MA_{0.16}) Pb(Br_{0.17}I_{0.83})₃ was used as an active layer for perovskite solar cell. From the results, it was observed that tandem device displayed 26.3% efficiency over an active area of 1.43 cm² [39].

1.3 Objectives of the Study

- 1.** Preparation of single inverted planar perovskite solar cells (SIPPSCs) based different types of perovskite films by spin coating technique.
- 2.** Fabrication of multijunction inverted solar cells (MJISCs) based perovskite solar cell as a top cell and c-Si solar cell as a bottom cell to improve the efficiency.